Generation of an O/W emulsion in a flow-focusing microchip: importance of wetting conditions and of dynamic interfacial tension

Jiupeng Du, Nelson Ibaseta, Pierrette Guichardon

Generation of an O/W emulsion in a flow-focusing microchip: importance of wetting conditions and of dynamic interfacial tension

Jiupeng Du, Nelson Ibaseta*, Pierrette Guichardon

Aix Marseille Univ, CNRS, Centrale Marseille, M2P2, Marseille, France

Abstract

To date, there is no information on the microfluidic emulsification of dibutyl adipate and n-butyl acetate in water. Since these solvents are very suitable for microencapsulation by interfacial polymerization, it is highly necessary to study the emulsification behavior of these solvents in microchannel. This work shows that the microfluidic emulsification of these solvents in water may fail to obtain stabilized flow regimes. This is due to droplet coalescence and wall wetting, even if a hydrophilic microchip is used. Hydrodynamic results show that squeezing and dripping regimes are especially affected because of the wall wetting by the dispersed phase. This difficulty can be circumvented by adding a surfactant (here Tween 80) into the aqueous phase. However, high surfactant concentrations (ten times the critical micelle concentration) should be used for the water-dibutyl adipate system. Indeed, comparison of flow maps for several surfactant concentrations seems to indicate that the dynamic interfacial tension is higher than the one expected (equilibrium), for surfactant concentrations lower than one hundred times the critical micelle concentration. The estimated diffusion time of Tween 80 is compared to the droplet formation time at different conditions. The choice of more appropriate dimensionless numbers to represent flow maps is also discussed.

Keywords: Flow regimes, Wetting, Surfactant, Dibutyl adipate, n-Butyl acetate, Droplet, Microfluidics

1. Introduction

Polyurea microcapsules have a very hard and dense shell with a high chemical and mechanical stability (Scarfato et al., 2007; Ji et al., 2010; Polenz et al., 2014). Thus, they have attracted much interest for protecting relevant core materials such as catalysts (Yu et al., 2003), phase-change materials (Cho et al., 2002; Liang et al., 2009; Zhan et al., 2016), and fragrances (Jacquemond et al., 2009).

*Corresponding author

Email address: nelson.ibaseta@centrale-marseille.fr (Nelson Ibaseta)

Their production begins by dissolving one of the reactants (isocyanate), in a relevant solvent such as an ester, a ketone or an aromatic hydrocarbon. Then this oil phase is emulsified by an aqueous phase to form an O/W emulsion. Then, another reactant (an amine) will be added into this emulsion. As a consequence, polycondensation happens between these two reactants at the interface of emulsion. Dibutyl adipate and n-butyl acetate were chosen to be the candidate solvents for isocyanate in this study because of their low toxicity ("green" solvents, Diogo et al. (2014, 2015)) and good miscibility with isocyanate.

However, conventional emulsification in a batch usually produce polydisperse droplets, eventually resulting in difficult control of the size distribution of microcapsules. In this case, microfluidic emulsification has been considered as a promising technique because it can ensure the production of monodispersed droplet templates. Therefore, microfluidic emulsification combined with fast interfacial polycondensation (forming solid film within a few milliseconds, Polenz et al. (2015)) makes this microencapsulation method more attractive, as a facile and highly efficient route for continuous production of monodispersed polyurea microcapsules (Lone et al., 2013; Polenz et al., 2014, 2015).

Nevertheless, there is still a lack of information about the flow maps obtained when dispersing the two solvents (dibutyl adipate and n-butyl acetate) in water by using a microfluidic device. Indeed, common used organic liquids for microfluidic emulsion studies such as silicone oil and mineral oil can not dissolve the isocyanate. Since dibutyl adipate and n-butyl acetate have a lower hydrophobicity than silicone or mineral oil, they could eventually wet (at least partially) the surface of the microchannel. This could lead to the advent of disordered regimes (Dreyfus et al., 2003). Furthermore, if the microencapsulation step takes place in the microchannel, the wetting of the microchannel surface may lead to polyurea formation on these surfaces; since polyurea is not soluble in most solvents, this deposit would become permanent. Moreover, it could exacerbate the wetting by the dispersed phase, leading to a vicious circle.

Generally, there are three methods for solving wetting problems of the dispersed phase within microfluidic devices: surfactants addition (Tostado et al., 2011; Bashir et al., 2014; Yao et al., 2018); surface treatment (Li et al., 2007; Roberts et al., 2012; Li et al., 2018); and employment of non-planar geometry (Rotem et al., 2012; Jose and Cubaud, 2014; Yoon et al., 2018). The first two methods focus on increasing the equilibrium contact angles. On the other side, using a non-planar geometry can increase the droplet velocity and thus the dynamic contact angle between dispersed phase and the surface of microchannel, which also leads to ordered formation of droplets even when the equilibrium contact angle is not favourable.

Until now, the organic solvents used in existing studies (**Table 1**) about dewetting by adding surfactants are not adaptable to dissolve isocyanates. Therefore, an exploration about wetting behaviours with dibutyl adipate and n-butyl acetate within microfluidic devices is highly necessary. This exploration of wetting behaviours should also take into account previous works concerning the importance of the dynamic interfacial tension in microfluidic droplet generation (Tostado et al., 2011; Yao et al., 2018).

When a fresh surface is created during the formation of a drop or a bubble, initially

the surface excess Γ of surfactants is initially less than the equilibrium value Γ_∞. Hence, these "vacant sites" cause a flux of surfactant molecules from the bulk to the developing interface (Eastoe and Dalton, 2000). Consequently, the dynamic interfacial tension at the fresh interface decay from σ_t to σ_{eq}, until Γ reaches its equilibrium value, Γ_∞. However, within microfluidic devices, the frequency of droplet generation is so high that surfactant molecules may not have time to be transferred to the developing droplet interface, and the dynamic interfacial tension may be higher than expected from static (after one minute equilibration) measurements. Therefore, to avoid the effects of dynamic interfacial tension during droplet formation, excessive amounts of surfactant, tens to hundreds of times higher than the critical micelle concentration (CMC), are usually used in previous studies (Xu et al., 2006, 2012; Wang et al., 2009).

Table 1: Previous works using surfactants to avoid wetting the microchannel surface with the dispersed phase

Wall material	**Dispersed phase**	**Continuous phase**	**Emulsion**	**Surfactant**	**Reference**
Glass	Tetradecane.	Water	O/W	Span 80	Dreyfus et al. (2003)
PMMA	n-octane	Water	O/W	SDS	Xu et al. (2006)
	Water	Mineral oil	W/O	Span 80	Wu et al. (2007)
	Water	Corn oil	W/O	CTAB	Tostado et al. (2011)
	Water+glycerol	Octane	W/O	Span80	Yao et al. (2018)
	Octane	Water+glycerol	O/W	SDS	
PDMS	Water	Mineral oil	W/O	Span 80	Bashir et al. (2014)

In the present work, these two special organic liquids are emulsified by water containing Tween 80 in a glass-made microchannel. The questions that this work wants to answer are thus the following: is there a partial wetting of the glass microchannel by the dibutyl adipate and n-butyl acetate dispersed phase and does it lead to a modification of the flow map? If the use of a surfactant is needed, should the dynamic interfacial tension be taken into account? We first map out different regimes of water-dibutyl adipate system in a hydrophilic flow-focusing microchannel and discuss the influence of wetting conditions on different regimes. Then, we show that the wall wetting by dibutyl adipate (dispersed phase) can be modified by adding a surfactant Tween 80 (HLB= 15.0) and the relationship between surfactant concentrations and dynamic interfacial tension is also studied. Finally, we use n-butyl acetate as the dispersed phase to study its wetting conditions (without and with surfactant) on different flow regimes and verify the consistency of its flow map with that of water-dibutyl adipate system.

2. Materials and Methods

2.1. Materials

The surfactant, Polyoxyethylenesorbitan monooleate (Tween 80, Sigma Aldrich, composition: oleic acid, 58.0%, balance primarily linoleic, palmitic, and stearic acids); dibutyl adipate (TCI, 99.9%); and n-butyl acetate (Across Organics, 99.4%), are used without additional purification. Distilled water is produced by mono-distillate 2008, GFL. All liquids are filtered by syringe filter (JVLAB, PTFE with 0.45 μm pore size), before being supplied into the microchannel.

Tween 80 (non-ionic surfactant) can be soluble in both aqueous and organic phases, which are confirmed by UV spectroscopy (**Figure S1**, given in the supplementary material). However, in this study, we dissolve Tween 80 in the aqueous phase and then make the emulsion within the microchannel. Considering the fast droplet formation (2ms–580ms) by microfluidics, the diffusion of Tween 80 into organic phases is probably negligible.

2.2. Physical properties

2.2.1. Density and viscosity

The density (ρ) is measured by an Anton Paar DMA 35 densimeter with an accuracy of $1 kg/m^3$. All the measurements are performed at $25 \pm 0.5^{\circ}C$; the viscosity (μ) of all used liquids at $25 \pm 0.5^{\circ}C$ is found in the literature (R.LIDE, 2009; Diogo et al., 2015; Szymczyk and Taraba, 2016), which are summarised in **Table S1** (See in the supplementary material). The comparisons of the measured values for different Tween 80 concentrations and those by Szymczyk and Taraba (2016), show relative errors lower than 0.01%.

2.2.2. Interfacial tension and contact angles after one minute equilibration

Contact angles (CA) and interfacial tension (σ) are measured after one minute equilibration by a tensiometer (Dataphysics OCA 20, resolution 0.01mN/m and 0.01 $^{\circ}$) with Sessile drop method and Pendant drop method, respectively. For the measurements of CA, the microchip is immersed in aqueous phase with different concentration of Tween 80. Five micro-liters of phase (d) is injected through an inverted needle, because dispersed phase is lighter than the continuous phase. The outer surface of the microchannel is used for measuring CA. In fact, for an uncoated microchip of Dolomite, the outer and inner surfaces are the same (borosilicate glass). Before every measurement of CA, the microchip is deposed in an ultrasonic bath containing 2wt% sodium dodecyl sulfate (SDS) solution, acetone and water for 5 minutes each. And then the microchip is dried by compressed air. For the measurements of interfacial tension, a 5 μL organic drop is formed in the aqueous phase. After one minute, the value of σ is taken. For both measurements, the Young-Laplace fitting is chosen to calculate the CA and σ values.

As presented in **Figure 1**, the equilibrium interfacial tension (σ) at $25 \pm 0.5^{\circ}C$, between distilled water and dibutyl adipate is measured to be 19.41mN/m. And the equilibrium interfacial tension between distilled water and n-butyl acetate is 14.12 mN/m, which is well consistent with the values presented by Donahue and Bartell (1952): 14.5 mN/m at $25 \pm 0.5^{\circ}C$. Then the interfacial tension of both systems (**Figure 1**, represented by $\triangle$ and

▲) sharply reduces by adding Tween 80 into aqueous phase until 0.01wt%, which is the CMC (critical micellar concentration) of Tween 80 in water. After this point, the interfacial tension slowly reduces with further addition of Tween 80. Eventually, with 1wt% of Tween 80 in water, the interfacial tension is reduced to 7.01 mN/m for dibutyl adipate and 6.36 mN/m for n-butyl acetate.

Firstly, the contact angle of water on the clean surface of microchip is measured to be $34.3 \pm 0.2^{\circ}$ at $25 \pm 0.5^{\circ}C$, which is consistent well with the values presented by Sumner et al. (2004), in presence of air. Both organic liquids partially wet the surface of microchip when no surfactant is added. The contact angles at $25 \pm 0.5^{\circ}C$, are 157.53° for water-dibutyl adipate system and 154.23° for water-n-butyl acetate, respectively. An opposite evolution is observed for contact angles of two organic phases on the surface of the microchip with the addition of Tween 80 (**Figure 1**, represented by ◇ and ◆). At above CMC, for both chemical systems, the contact angles increase up to an angle close to 180°. When the contact angles reach this level, the formed drop would detach from the surface and finally float on the surface of water. In this case, aqueous phase completely wet the surface of the microchip.

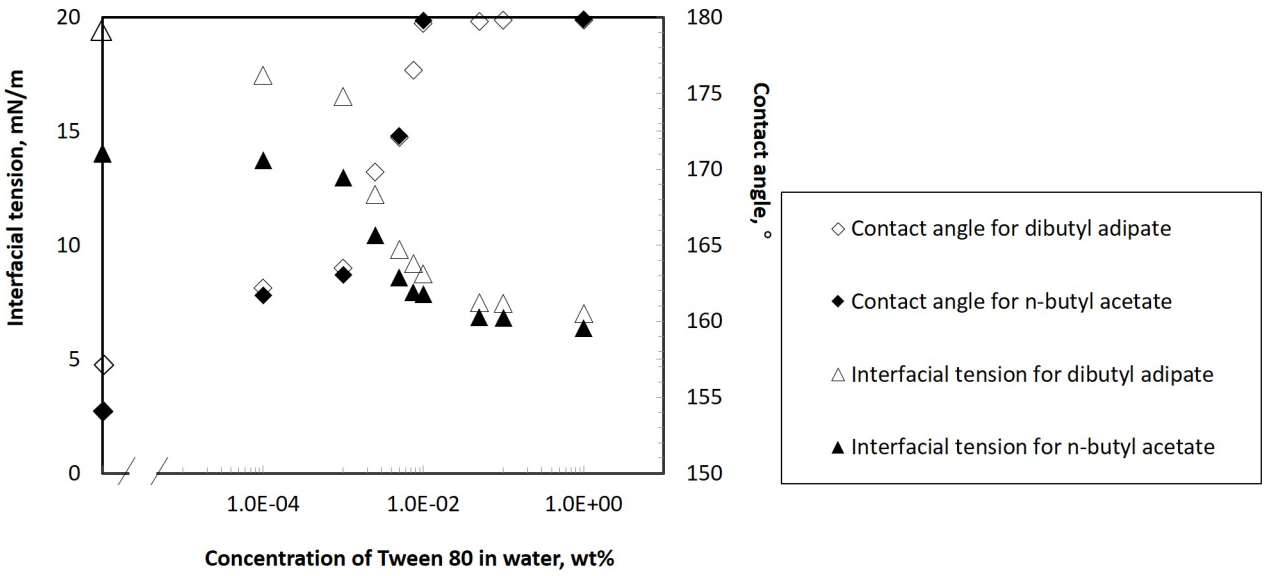

Figure 1: The interfacial tension between distilled water and organic liquids and contact angles measured after 1 min equilibration, at varying surfactant concentrations of Tween 80 and at $25 \pm 0.5^{\circ}C$.

2.3. Experimental set-up

We perform the experiments in a hydrophilic microchip made of borosilicate glass (Droplet Junction Chip, Dolomite Microfluidics ©, UK) during the preparation of an O/W emulsion. The geometry of chip is named flow-focusing with junction width $105\mu m$, wide channel width $300\mu m$ and overall height $100\mu m$, as presented in **Figure 2(a)**.

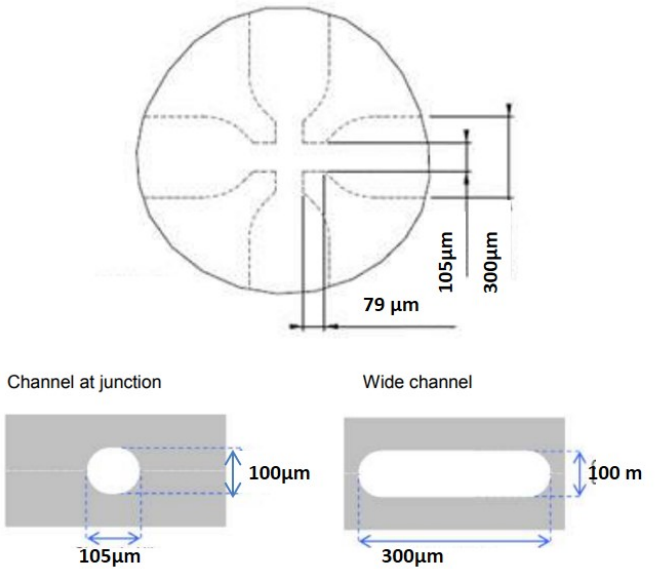

(a)

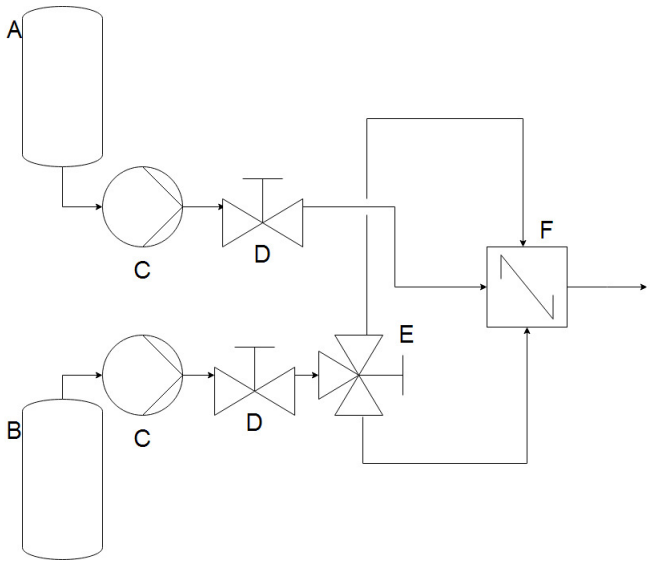

(b)

Figure 2: (a). Microfluidic chip geometry. Reprinted with permission from the Dolomite Product Datasheet. (b). Schematic diagram of the microfluidic set-up. A - tank of dispersed phase; B - tank of continuous phase; C - pressure pumps; D - valves; E - three-way connector; F - microchip.

The feeding of the aqueous and organic phases is realized by using two pressure pumps (Mitos P-Pump, response time <4s, Dolomite Microfluidics ©, UK), equipped with two types of flow rate sensors (Mitos Flow Rate Sensors of 0.2–7μL/min for the dispersed phase and 6-1000μL/min for the continuous phase, response time <30ms, Dolomite Microfluidics ©, UK). The droplet formation and flow regimes are visualized using a high-speed camera with a built-in microscope (Meros High Speed Digital Microscope, 4000fps, Dolomite

Microfluidics ©, UK). The entire experimental set-up is presented in **Figure 2(b)**.

2.4. Experimental method

According to the static measurements of interfacial tension, at a concentration of Tween 80 above 0.01 wt% (CMC), the interfacial tension is only slightly affected by a further addition of surfactant (8.73mN/m for 0.01 wt%, 7.45mN/m for 0.1 wt% and 7.01mN/m for 1 wt% respectively). The same behaviour is obtained for equilibrium contact angles, as they approach a value of 180° (no wetting problem under static conditions) for the three concentrations. We firstly perform the study with water-dibutyl adipate system to show the wetting influence of dispersed phase on different regimes. Then, we have obtained the flow maps for three different concentrations (CMC, 10 CMC and 100CMC) of Tween 80 aqueous solution and dibutyl adipate, for exploring the relationship between dynamic interfacial tension and concentration of Tween 80. Finally, another organic phase n-butyl acetate is also studied with and without Tween 80, for the reason that it has similar interfacial tension and contact angles as dibutyl adipate but a different viscosity.

Experiments are carried out at constant (controlled) volumetric flow rates of the dispersed phase (Q_d) and continuous phase (Q_c). After any change in the flow rate, film acquisition is switched on after a stabilisation period of at least one minute.

After each experiment, a cleaning protocol is carried out as follows: firstly, a 2wt% sodium dodecyl sulfate (SDS) aqueous solution flows to the microchannel for at least 30 minutes; then distilled water and acetone are introduced to the microchip for further cleaning the surface of microchannel, respectively; finally, the microchannel is dried by compressed air.

Experiments in the results section are described as a function of the Capillary numbers (Ca) or Weber numbers (We),

$$Ca = \frac{u\mu}{\sigma} = \frac{\text{Viscous forces}}{\text{Interfacial forces}} \tag{1}$$

$$We = \frac{\rho u^2 L}{\sigma} = \frac{\text{Inertial forces}}{\text{Interfacial forces}} \tag{2}$$

where the characteristic velocities used for these estimations are the average velocities ($u_d = Q_d/A$, $u_c = Q_c/A$, m/s) at the junction of microchannel in **Figure 2(a)**, and A is the cross-sectional surface at the junction which can be considered as a circle combined with a small rectangular ($A = \pi \times 50^2 + 5 \times 100 = 8.35 \times 10^3 \mu m^2$). The hydraulic diameter L ($L = 4A/(2\pi \times 50 + 5 \times 2) = 103\mu m$) at the junction, is chosen as a characteristic length scale.

3. Results

3.1. Flow map for the water-dibutyl adipate system

The flow map for the water-dibutyl adipate system is shown in **Figure 3**. The values of Ca_c and Ca_d are in the range of $1.0 \cdot 10^{-3} < Ca_c < 3$, $0 \cdot 10^{-2}$ and $1.0 \cdot 10^{-3} < Ca_d < 1.0 \cdot 10^{-2}$,

respectively. Six different flow regimes are observed for this system in the microchannel: disordered squeezing, ordered squeezing, disordered dripping, dripping, jetting and threading.

Because of the partial wetting of dibutyl adipate, part of squeezing is replaced by disordered squeezing at very low flow rates of both phases. By increasing the flow rate of dispersed phase, the transition from disordered squeezing to ordered squeezing is attained. Further accelerating the dispersed phase can produce a more important inertial force, which leads to a transition of squeezing to jetting or threading. On the other hand, by increasing the flow rate of continuous phase can induce a transition from squeezing to dripping as a result of a more important external shear stress overcoming of interfacial tension. Also, because of the partial wetting of dispersed phase, the disordered dripping is obtained when the flow rate of continuous phase is not high enough. In general, two critical capillary numbers ($Ca_d > 6.0 \times 10^{-3}$ or $Ca_c > 1.0 \times 10^{-2}$) can be obtained from **Figure 3**, where the wetting conditions are not important even if there is partial wetting of dispersed phase on the surface of microchannel.

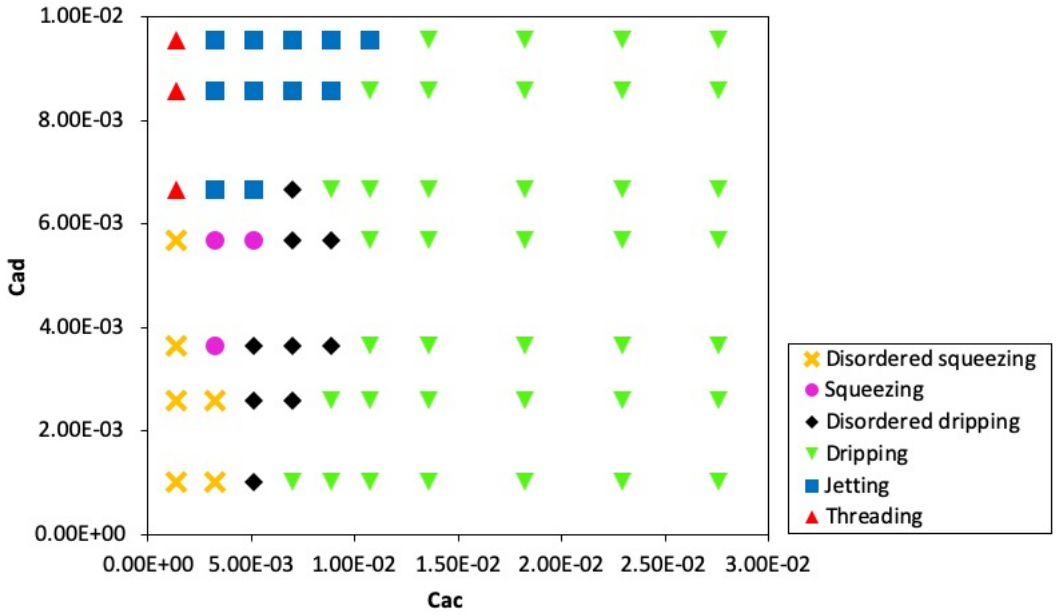

Figure 3: Flow map for water-dibutyl adipate system. Flow rates of dispersed phase: $2 - 19\mu L/min$; Flow rates of continuous phase: $15 - 300\mu L/min$.

3.2. Different flow regimes for the water-dibutyl adipate system

In this section, all the different flow regimes are discussed in detail.

3.2.1. Squeezing regime

When the flow rate of the continuous phase is small, the squeezing regime (disordered and ordered) is observed: the large droplet obstructs the cross-section of wide channel and

finally broke up because of increased pressure of continuous phase upstream(Romero and Abate, 2012).

1) Disordered squeezing regime

Disordered squeezing regime happens when both capillary numbers are extremely small ($Ca_d < 5.7 \cdot 10^{-3}$ & $Ca_c < 3.2 \cdot 10^{-3}$), which gives the droplets with different size and shape. This non-classic regime is due to the partial wetting of the microchip by the dispersed phase.

Firstly, the growing droplet arrives at a size comparable to the thickness ($100\mu m$) of microchannel, it wets the upper and bottom surfaces of the microchannel (**Figure 4(a)**). In the next stage, the growing droplet adheres to the left and right sides (**Figure 4(b)**) of the microchannel. When the growing droplet obstructs the channel the continuous phase accumulates and increases its pressure. Once this pressure is high enough, the continuous phase pinches off the droplet (**Figure 4(c)**).

These formed droplets move very slowly under such low flow rates of the continuous phase after the detachment, which can not provide enough distance among them. Besides, the velocity's field near the junction and the pressure in two fluids can be modified by these slow-moving droplets. Consequently, droplets with different size and different distance are produced. Formed droplets are very close and can get in contact within microchannel. As there is no surfactant's protection, coalescence of these droplets can happen.

2) Ordered squeezing regime

The ordered squeezing regime is obtained at slightly larger capillary numbers ($3.2 \cdot 10^{-3} < Ca_c < 5.1 \cdot 10^{-3}$, $3.7 \cdot 10^{-3} < Ca_d < 5.7 \cdot 10^{-3}$), by increasing the flow rates of two phases.

Although those large droplets contact directly with the confining walls of microchannel, it seems that a higher shearing stress can easily force the formed droplet to move downstream. As a consequence, it does not influence the flow field near the junction and ensure the formation of droplets regularly with the same size and fixed distance. However, because of partial wetting, there is some trace of dispersed phase left on the surface of microchannel when it moves, as shown in **Figure 4(d)**.

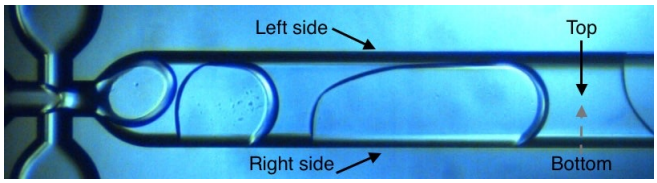

(a)

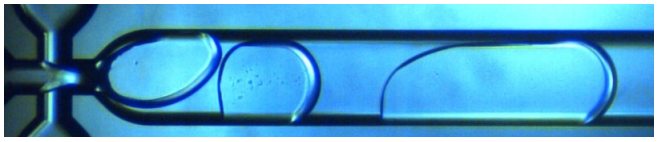

(b)

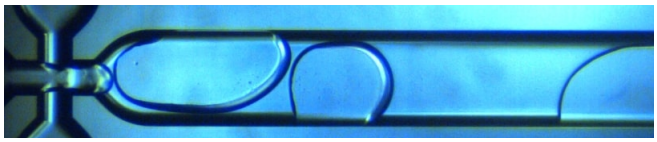

(c)

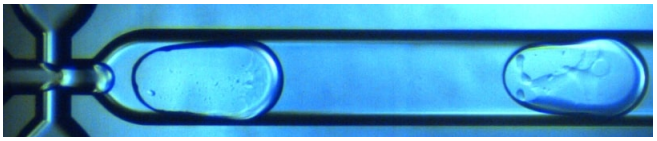

(d)

Figure 4: Mechanism of droplet formation within disordered and ordered squeezing regime with a water-dibutyl adipate system. (a)-(c). Different stages of droplet formation for disordered squeezing regime at $u_c = 0.030m/s$, $u_d = 0.010m/s$, $Ca_c = 1.3 \cdot 10^{-3}$, $Ca_d = 2.6 \cdot 10^{-3}$. (d). Ordered squeezing regime at $u_c = 0.070m/s$, $u_d = 0.015m/s$, $Ca_c = 3.2 \cdot 10^{-3}$, $Ca_d = 3.7 \cdot 10^{-3}$.

3.2.2. Dripping regime

By increasing flow rate of the continuous phase, a more important shearing stress by continuous phase is achieved. The drops are formed inside or near the junction of microchannel, and eventually pinch off due to an absolute stability (Utada et al., 2008). Also because of the partial wetting of dispersed phase on the surface of microchannel, dripping is not stable at low flow rates of continuous phase.

Indeed, when this flow rate is not high enough, the diameter of the droplet is equal to the height of the microchannel. The velocity of the droplet decreases after the junction, because the microchannel become wider. Therefore, the new droplet reaches the previous one (**Figure 5(a)**). Since there is no surfactant's protection, the two droplets merge into a larger droplet (**Figure 5(b)**). This larger droplet is more likely to adhere to the surface of the microchannel because of a larger contact area with the surface of microchannel, causing fusion with the droplets formed later (**Figure 5(c)**).

Figure 5(c) to **5(e)** illustrate the evolution of disordered dripping to ordered dripping by increasing the flow rate of the continuous phase. Formation of droplets becomes more and more stable with the flow rate of the continuous phase.

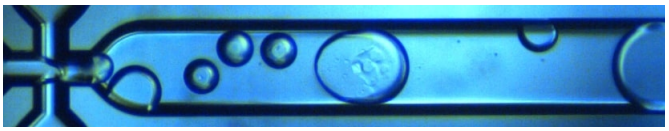

(a)

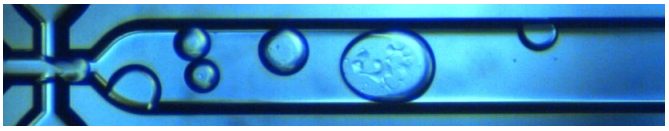

(b)

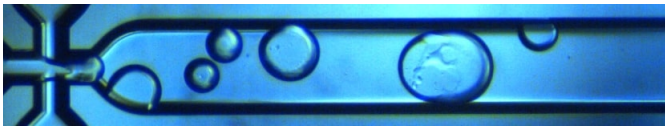

(c)

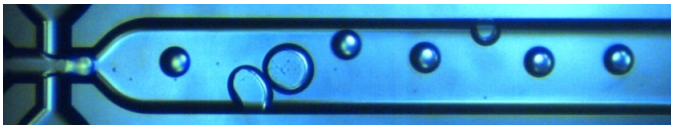

(d)

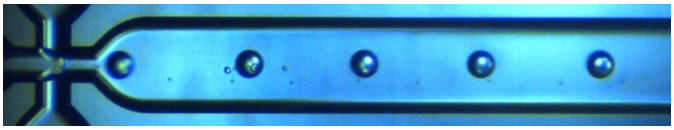

(e)

Figure 5: Disordered and ordered dripping regimes at different flow conditions with a water-dibutyl adipate system: (a)-(c). Mechanism of droplet formation within disordered dripping regime at $u_c = 0.111m/s$, $u_d = 0.010m/s$, $Ca_c = 5.1 \cdot 10^{-2}$, $Ca_d = 2.6 \cdot 10^{-3}$; (d). Disordered dripping regime at $u_c = 0.152m/s$, $u_d = 0.010m/s$, $Ca_c = 7.0 \cdot 10^{-2}$, $Ca_d = 2.6 \cdot 10^{-3}$; (e). Ordered dripping regime at $u_c = 0.234m/s$, $u_d = 0.010m/s$, $Ca_c = 1.1 \cdot 10^{-2}$, $Ca_d = 2.6 \cdot 10^{-3}$.

3.2.3. Jetting regime

By increasing the flow rate of the dispersed phase, a jetting is formed (**Figure 6**) and the drop pinches off downstream due to a convective instability (Utada et al., 2008). When the inertial force of dispersed phase and the shearing force of continuous phase are large enough to overcome the interfacial tension (the only force holding the dispersed phase inside the junction), the dispersed phase is dragged downstream before the instability arrives at the critical value needed to break up the droplet.

This regime is not influenced by the wetting of the dispersed phase on the surface of microchannel. This observation is because the jetting regime only happens at very high flow rates of both phases. Therefore, the formed droplets are dewetted from the surface of microchannel by the high shearing force of the continuous phase.

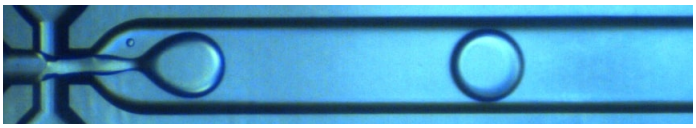

Figure 6: Jetting regime at $u_c = 0.30m/s$, $u_d = 0.044m/s$, $Ca_c = 1.4 \cdot 10^{-2}$, $Ca_d = 1.1 \cdot 10^{-2}$, with a water-dibutyl adipate system.

3.2.4. Threading regime

Keeping a low flow rate of the continuous phase and further increasing the flow rate of the dispersed phase, a thread can be formed (**Figure 7**), which is confined at the top and bottom surface of microchannel. Within this regime, no pinch-off of droplets within microchannel is observed.

As can be seen from **Figure 7(a), 7(b)**, the thread of dispersed phase adheres either to the left side or right side of the wide channel. This is also caused by the partial wetting of dispersed phase on the surface of the microchannel, which is not regular during the operation.

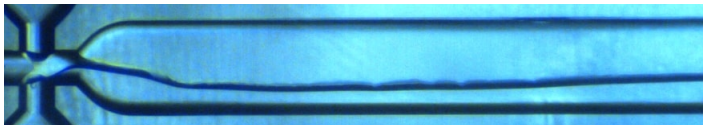

(a)

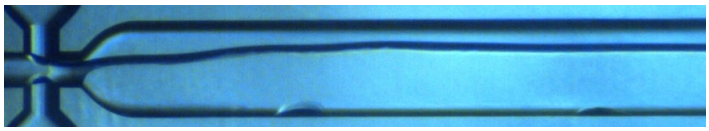

(b)

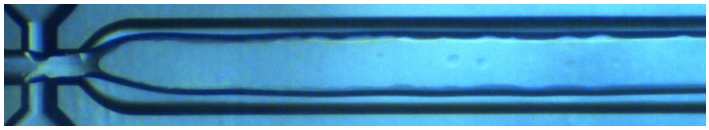

(c)

Figure 7: Threading regime at different flow conditions with a water-dibutyl adipate system: (a). $u_c = 0.030m/s$, $u_d = 0.027m/s$, $Ca_c = 1.3 \cdot 10^{-3}$, $Ca_d = 6.7 \cdot 10^{-3}$; (b). $u_c = 0.030m/s$, $u_d = 0.038m/s$, $Ca_c = 1.3 \cdot 10^{-3}$, $Ca_d = 9.6 \cdot 10^{-3}$; (c). $u_c = 0.030m/s$, $u_d = 0.044m/s$, $Ca_c = 1.3 \cdot 10^{-3}$, $Ca_d = 1.1 \cdot 10^{-2}$.

3.3. Influence of surfactant on the flow maps for water-dibutyl adipate systems

Figure 8 shows the flow maps for the water-dibutyl adipate system when Tween 80 is added to the aqueous (continuous) phase. All the Capillary numbers are calculated by using the measured interfacial tension presented in **Figure 1**. Since the interfacial tension falls to 40% of that without surfactant, lower flow rates of both phases are used to obtain flow maps with the same orders of magnitude of the Capillary numbers.

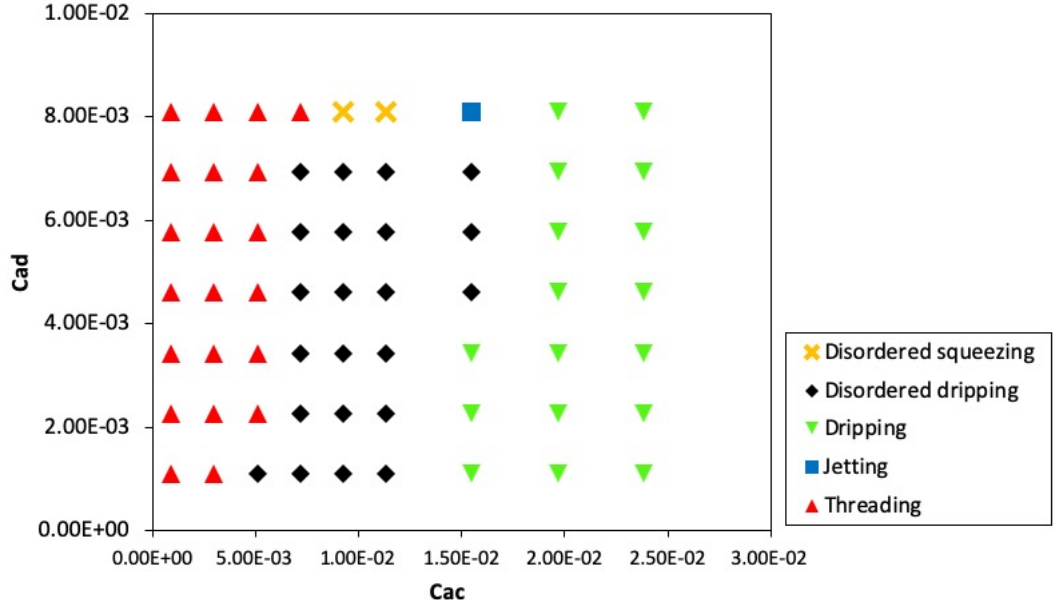

(a)

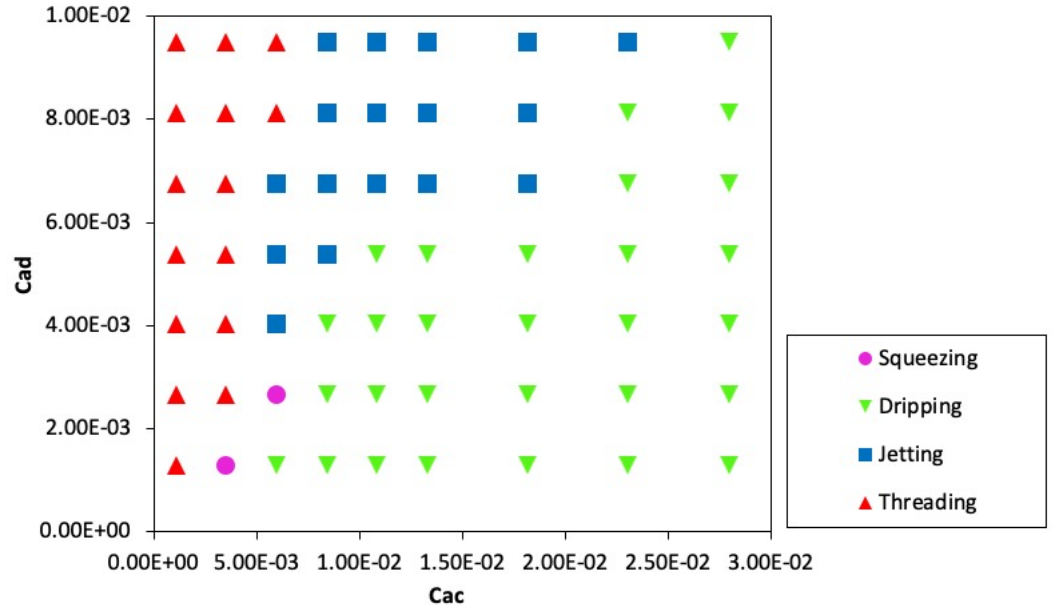

(b)

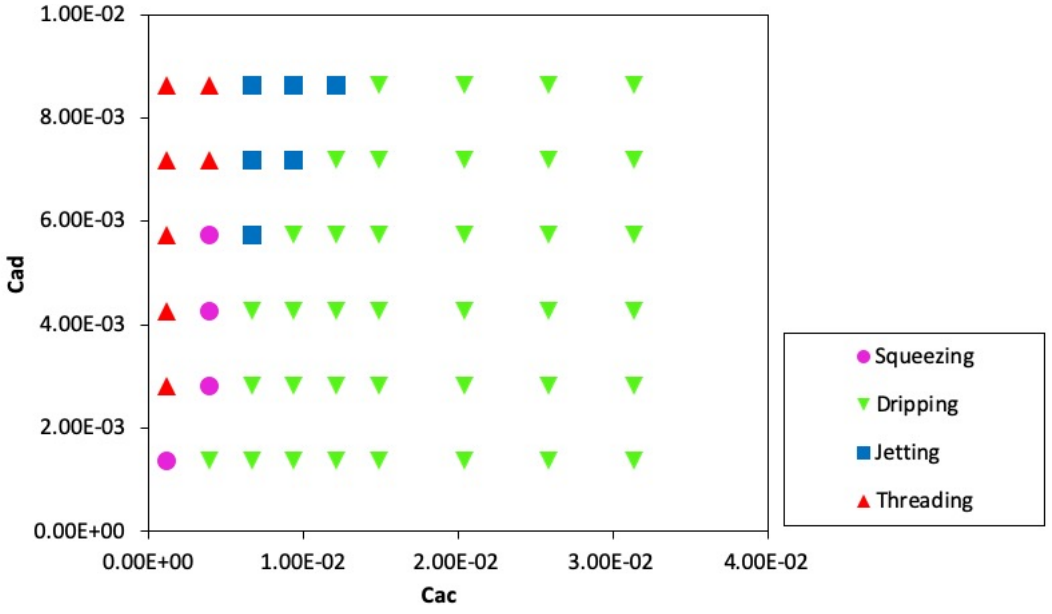

(c)

Figure 8: (a). Flow map for CMC of Tween 80 aqueous solution-dibutyl adipate. (b). Flow map for 10 CMC of Tween 80 aqueous solution-dibutyl adipate. (c). Flow map for 100 CMC of Tween 80 aqueous solution-dibutyl adipate. The flow rates of dispersed phase: $1-7\mu L/min$; The flow rates of continuous phase: $4-96\mu L/min$.

The addition of Tween 80 at its CMC reduces the region of disordered regimes, as it can be observed in the flow maps (**Figure S2**) given in the supplementary material. When the Capillary numbers are used to draw the flow map (**Figure 8(a)**), it can be seen that all the regime transitions happen at larger Ca_c and Ca_d. This could be explained by an underestimation of the interfacial tension (see the Discussion section below).

Further addition of Tween 80 with a concentration of 10 CMC into distilled water, eliminates the disordered flow regimes, as shown in **Figure 8(b)**. However, the transition of different regimes on the flow map for 0.1wt% Tween 80-dibutyl adipate system, still occurs at larger values of apparent Ca_c than that of a surfactant-free system.

Finally, when the concentration of Tween 80 is 100 times the CMC, the flow regime transitions (**Figure 8(c)**) are observed at values of capillary number very close to those of the surfactant-free system.

3.4. Flow maps for the water-n-butyl acetate systems

In this section, n-butyl acetate which is less viscous than dibutyl adipate, is used as a dispersed phase. Except for this difference, both organic liquids have very close evolution of contact angles and interfacial tension at the same concentration of Tween 80 (see **Figure 1**).

There are also disordered flow regimes caused by partial wetting of n-butyl acetate (**Figure 9(a)**), when no surfactant is added into the aqueous phase. To verify the influence of surfactant on dynamic wetting behaviours of n-butyl acetate within microchannel, a 1 wt% of Tween 80 aqueous solution is used as continuous phase. Like water-dibutyl adipate, the disordered regimes could be eliminated by adding 1 wt% of Tween 80 into aqueous phase. And the flow map with 1 wt% of Tween 80 (**Figure 9(b)**) is well consistent with that without adding Tween 80.

However, the flow maps for n-butyl acetate are noticeably different to those with dibutyl adipate. Apparently, jetting regime occurs at much smaller values of Ca_d for n-butyl acetate. This observation makes us wonder about the appropriate use of Ca_d when characterising flow regimes transition in the case of different chemical dispersed phases.

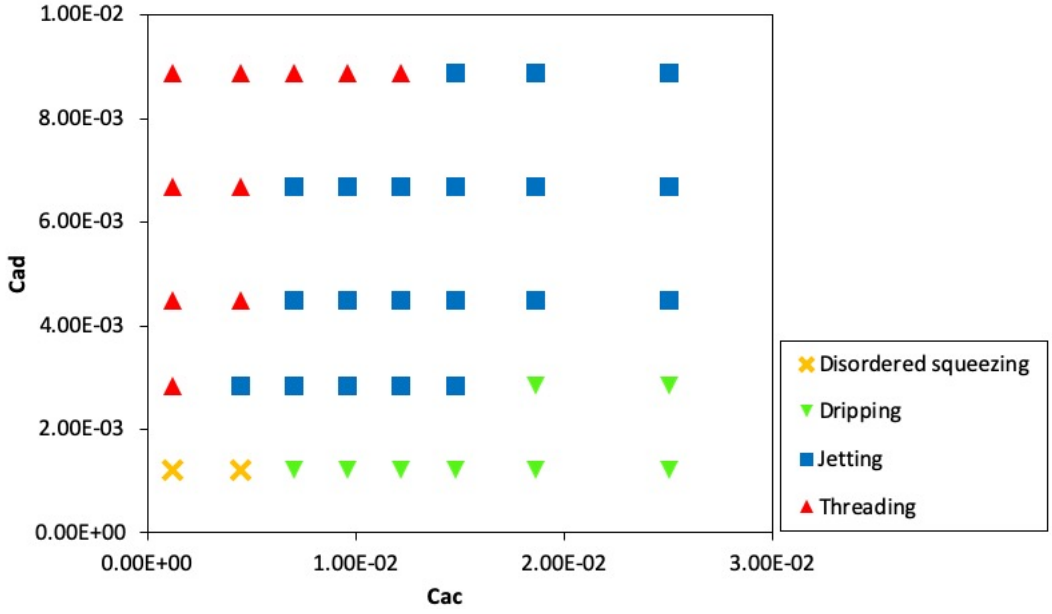

(a)

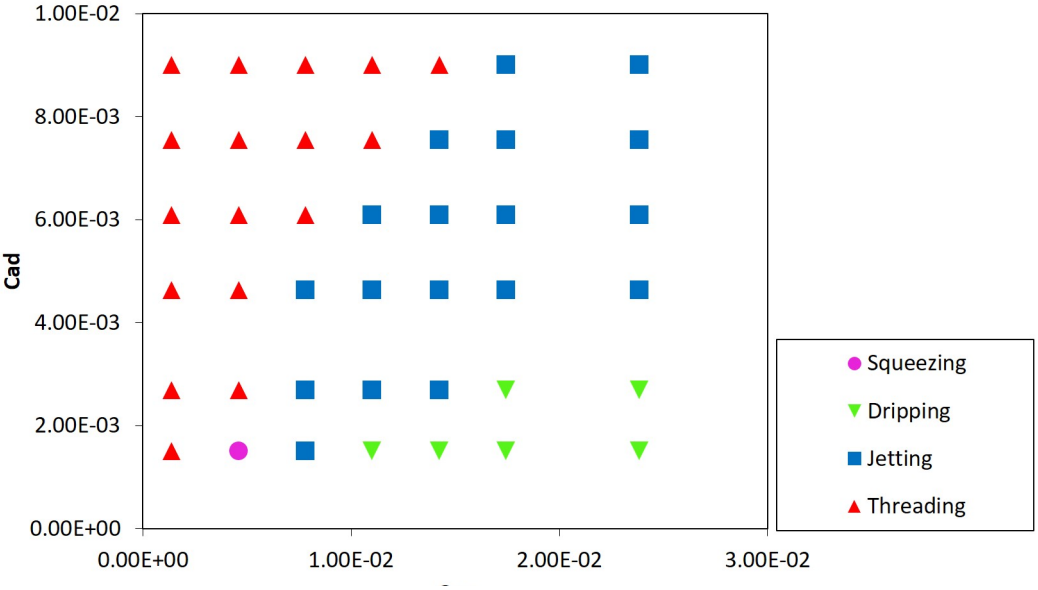

(b)

Figure 9: (a). Flow map for water-n butyl acetate system. (b). Flow map for 1 wt% of 100 CMC of Tween 80 aqueous solution-n butyl acetate system. The flow rates of dispersed phase: $12-92\mu L/min$ for (a) and $7-42\mu L/min$ for (b); The flow rates of continuous phase: $10-200\mu L/min$ for (a) and $4-76\mu L/min$ for (b).

4. Discussion

4.1. Importance of dynamic interfacial tension

The flow maps (**Figure 8**) for Tween 80 (aq)-dibutyl adipate systems, show that the different flow regimes do not match with those without surfactant (**Figure 3**). Only when the concentration is at 100 CMC, the transition of dripping to jetting is close to that of a surfactant-free system. This observation may indicate that the interfacial tension is underestimated and thus the capillary numbers are overestimated. One explanation is that the interfacial tension is measured after 1 min equilibration, whereas droplet generation is a dynamic process with small characteristic time.

In fact, the frequency of formation of the drops within a microfluidic device is so high that it may not allow the Tween 80 to diffuse into the new interface. When the concentration of surfactant is above CMC (our cases in this study), there are three steps for the adsorption of surfactant on the new interface: the transport of the free molecules and micellars of surfactant, through the boundary layer; the adsorption of free surfactant molecules onto the interface and the disaggregation of micellars at the boundary layer; and finally the rearrangement of the adsorbed molecules on the interface into an equilibrium state (Chen and Neumann, 1998; Xu et al., 2012).

By adding more Tween 80 (much more than CMC), an increased number density of micellars in the continuous phase creates a larger concentration gradient for the first step above (Wang et al., 2009), which would enhance the mass transfer of micellars into the boundary layer. Therefore, for the concentrations of Tween 80 at CMC, 10 CMC and 100 CMC, the dynamic interfacial tension with 100 CMC of Tween 80 in continuous phase, would be more close to the equilibrium value.

4.1.1. Film theory for estimating the characteristic transport time of Tween 80 molecules

To estimate the characteristic transport time for three surfactant concentrations used in this study, a film theory model is used to describe the mass transfer of Tween 80 molecules from the aqueous phase to the new interface in microchannel.

This characteristic time scale can be estimated by (Paria and Khilar, 2004),

$$\tau = \frac{\delta^2}{D} \tag{3}$$

where δ is the thickness of the film (boundary layer) across which diffusion occurs and D is the diffusion coefficient.

4.1.2. Effective diffusion coefficient

In our study, three concentrations used are at or over CMC. Therefore, the contribution of micellars in the surfactant transport should also be considered. Based on the assumption that micellization kinetics are fast compared to diffusion for Tween 80 (Joos and Uffelen, 1995; Glawdel and Ren, 2012; Kovalchuk et al., 2018), an effective diffusion coefficient (D_{eff}) including the effects of micellars can be represented as

$$D_{eff} = \frac{Dc_0}{CMC}\left[1 + \left(\frac{c_0}{CMC} - 1\right){N_a}^{-2/3}\right] \tag{4}$$

where c_0 is the concentration of surfactants in the solution, mol/m^3 and N_a is the aggregation number of micellars. For Tween 80, N_a is found to be 22 at $25^{\circ}C$ (Glenn et al., 2005). D is the diffusion coefficient of Tween 80 monomers, which is reported to be $5.1 \times 10^{-11} m^2/s$ at $25^{\circ}C$ (Léonard-Akkari et al., 2018). CMC is taken from our measurement as $0.076 mol/m^3$ at $25^{\circ}C$. All these parameters are constant for three concentrations used in this study. And D_{eff} for three concentrations (CMC, 10 CMC and 100 CMC) are calculated as $5.1 \times 10^{-11} m^2/s$, $1.1 \times 10^{-9} m^2/s$ and $7.0 \times 10^{-8} m^2/s$, respectively. Replacing D by D_{eff} in **Equation 3** results in

$$\tau = \frac{\delta^2}{D_{eff}} \tag{5}$$

4.1.3. Thickness of boundary layer

According to the film theory, a thin stagnant film (boundary layer) exists on either side of the interface. And mass transfer through this film is regarded as affected only by molecular diffusion. Therefore, the thickness (δ) of this hypothetical film can be calculated as (Doran, 2013),

$$\delta = \frac{D_{eff}}{k_c} \tag{6}$$

where k_c is the convective mass-transfer coefficient.

Sherwood number Sh represents the ratio of the convective mass transfer to the rate of diffusive mass transport,

$$Sh = \frac{k_c}{D_{eff}/L} \tag{7}$$

where L ($103 \mu m$) is the hydraulic diameter at the junction. Substituting **Equation 6** into **Equation 7**, the thickness of the boundary layer is estimated to be,

$$\delta = \frac{L}{Sh} \tag{8}$$

4.1.4. Characteristic transport time of Tween 80 at different conditions

The transport of Tween 80 molecules can take place by diffusion and convection. To get an idea of a characteristic order of magnitude, we consider that there are two limiting cases: the limiting case where transport takes place only by molecule diffusion and the limiting case where convection is predominant.

When the droplet is under static situation (mainly pure molecule diffusion), the thickness of the boundary layer is

$$\delta_1 = \frac{L}{Sh} = \frac{L}{2} \tag{9}$$

where Sherwood number equals 2 for natural convection and molecule diffusion to a single spherical particle (Ranz and Marshall, 1952). The maximum characteristic transport time, τ_{max} is given as,

$$\tau_{max} = \frac{\delta_1^2}{D_{eff}} = \frac{L^2}{4 D_{eff}}. \tag{10}$$

When forced convection dominates the transfer of Tween 80 molecules, the minimum characteristic transport time, τ_{min} is given as,

$$\tau_{min} = \frac{\delta_2^2}{D_{eff}} \tag{11}$$

where δ_2 is the thickness of the boundary layer at the highest average velocity ($0.23m/s$) of the continuous phase in this study.

For the forced convective mass transfer of species into liquid streams, the Sherwood number is correlated (Welty et al., 1969) as,

$$Sh = (4 + 1.21Pe^{2/3})^{1/2} (Pe < 10000) \tag{12}$$

or

$$Sh = 1.01Pe^{1/3} (Pe > 10000) \tag{13}$$

Pe is the Peclet number outside the droplet,

$$Pe = \frac{u_c L}{D_{eff}} \tag{14}$$

where u_c is the average velocity of continuous phase. The thickness of boundary layer for forced convective mass transfer is,

$$\delta_2 = \frac{L}{Sh} = \frac{L}{(4 + 1.21Pe^{2/3})^{1/2}} (Pe < 10000) \tag{15}$$

or

$$\delta_2 = \frac{L}{Sh} = \frac{L}{1.01Pe^{1/3}} (Pe > 10000) \tag{16}$$

Considering all the influences (micellars, diffusive or convective mass transfer) on the transfer of surfactant, the estimated characteristic transport time of Tween 80 is summarized in **Table 2**.

Table 2: Estimated characteristic transport time (τ_{max}, τ_{min}) of Tween 80 molecules and droplet formation time (τ_{max-e}, τ_{min-e}) at different conditions.

Liquid	D_{eff}, m^2/s	τ_{min}, s	τ_{max}, s	τ_{min-e}, s	τ_{max-e}, s
0.01wt% (CMC) Tween 80 aqueous solution-dibutyl adipate	5.1×10^{-11}	3.4×10^{-2}	5.2×10^{1}	3.4×10^{-3}	3.4×10^{-2}
0.1wt% (10 CMC) Tween 80 aqueous solution-dibutyl adipate	1.1×10^{-9}	1.2×10^{-2}	2.4	3.2×10^{-3}	3.3×10^{-1}
1wt% (100 CMC) Tween 80 aqueous solution-dibutyl adipate	7.0×10^{-8}	2.4×10^{-3}	3.8×10^{-2}	2.8×10^{-3}	5.8×10^{-1}
1wt% (100 CMC) Tween 80 aqueous solution-n butyl acetate	7.0×10^{-8}	2.4×10^{-3}	3.8×10^{-2}	1.8×10^{-3}	1.2×10^{-1}

The maximum droplet formation time (τ_{max-e} in **Table 2**) corresponds to the minimum velocities of continuous and dispersed phases where the droplet can be successively generated in the microchannel. Whereas, the minimum droplet formation time (τ_{min-e} in **Table 2**) is obtained under the maximum velocities of the continuous and dispersed phases where the droplet is within the dripping regime. As for the widen jetting regime (big droplets) at higher velocity of the dispersed phase, its droplet formation time is not smaller than the smallest one within the dripping regime in this study.

It is obvious that only at 100 CMC of Tween 80 is the newly formed interface completely saturated by the surfactant in the microchannel, because the overall droplet formation time is higher than that estimated by Film theory. However, for the concentration at 10 CMC (or CMC) of Tween 80, the range of droplet formation time at different flow conditions is an order (or two orders) of magnitude lower than that estimated by Film theory.

These results are consistent with those of Wang et al. (2009), who observed a similar behaviour for Tween 20 aqueous solutions. Indeed, the physical properties of Tween 20 and Tween 80 are very similar.

4.2. Importance of wetting conditions on the fabrication of microcapsules

Although the essential part of this work concerns the influence of wetting on the flow maps, this is not the only effect on the success of the microfluidic emulsification. In fact, it can have some consequences on the cleaning protocol of microchip.

When no surfactant is used, it is necessary to avoid the wetting by the walls of microchannel and thus the disordered and even ordered squeezing regime should be avoided. Using dibutyl adipate as a dispersed phase causes difficulty for cleaning the microchip. This is because the dibutyl adipate is viscous (4.85cp at $25 \pm 0.5^{\circ}C$) and can partially wet the surface of microchannel, and thus it is very hard to remove it from the surface of microchannel just by flowing some common cleaning liquids such as acetone or propanol. To remove the residues of dibutyl adipate on the surface of microchannel, we had to change our cleaning protocol by flowing a 2wt% SDS solution through microchannel for at least 30 minutes before cleaning it by water and acetone. On the other hand, ordered dripping regime can be taken for the encapsulation process as it does not cause wetting of dispersed phase on the surface of microchannel. Also, within this regime, formed droplets are very monodispersed.

Alternatively, adding enough surfactant (e.g. 100 CMC for Tween 80) into the system, can well eliminate the wetting problem of dispersed phase. Besides, through this method, it can also help to obtain different sizes and shapes of droplets within different flow regimes.

4.3. Comparison of obtained flow maps with those in the literature

We compared our results with those realized in a similar geometry. Our flow map (**Figure 3**) of water-dibutyl adipate, is compared with that (**Figure S5**, given in the supplementary material) of silicone oil-water/glycerol in Kovalchuk et al. (2018), because both chemical systems have viscous dispersed phases (dibutyl adipate: 4.85 cp; water/glycerol: 6.00 cp). It is obvious that the dripping, jetting or threading of both chemical systems occurred at almost the same values of Ca_d and Ca_c. Except that, the disordered squeezing and disordered dripping existing in our system of water-dibutyl adipate does not happen for their system of water/glycerol-silicone oil. In fact, the system of water/glycerol-silicone oil does not have any wetting problem (Zhu and Wang, 2017), so it is often used for many studies concerning about microfluidic emulsification(Fu et al., 2012; Glawdel et al., 2012; Zhu et al., 2015). Generally, a good agreement of flow maps for dibutyl adipate with the literature is obtained.

However, the flow map (**Figure 9**) for n-butyl acetate, is noticeably different to that (**Figure 3**) for dibutyl adipate. For example, the jetting regime occurs at very small Ca_d values ($Ca_d > 2.2 \cdot 10^{-3}$) when n-butyl acetate is used as dispersed phase, whereas jetting regime does not happen until $Ca_d > 1.1 \cdot 10^{-2}$ for a water-dibutyl adipate system. This observation might reveal a fact that the capillary number (viscous effects over interfacial tension) of dispersed phase, is not enough to identify the flow maps among different chemical systems within the same microchannel. The inertia effects (Weber number) of dispersed phase, might not be negligible according to types of dispersed phases.

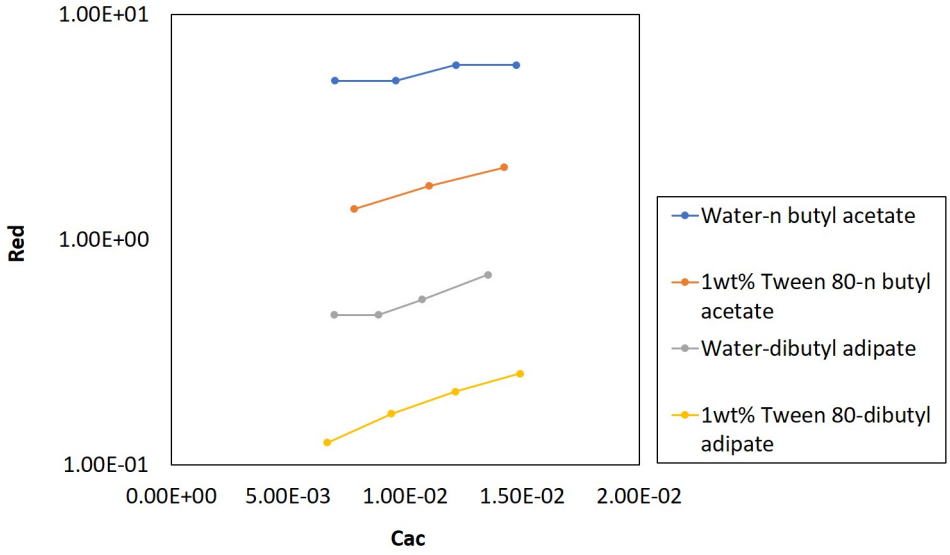

(a)

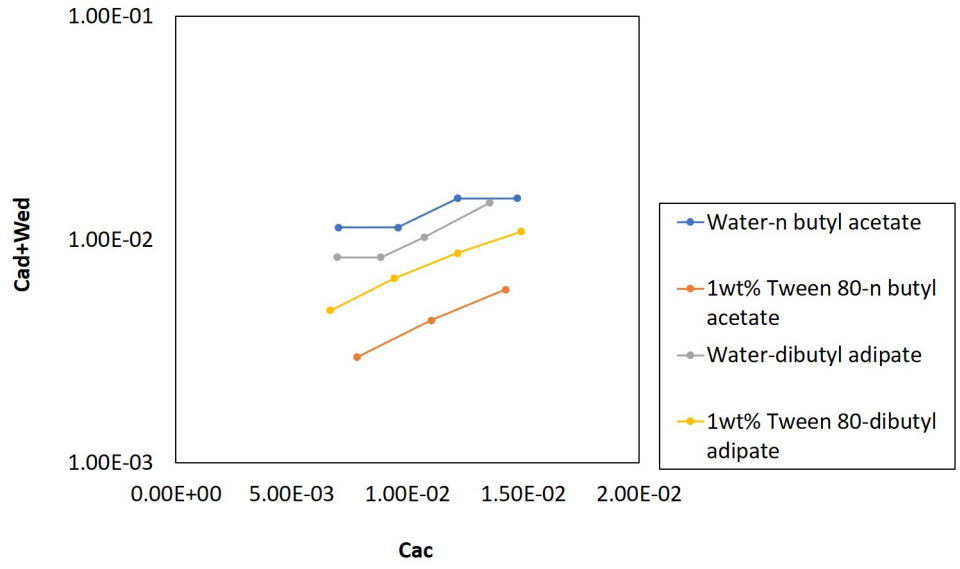

(b)

Figure 10: (a). Flow regime transition from dripping to jetting regime represented by Re_d and Ca_c. (b). Flow regime transition from dripping to jetting regime represented by $(Ca_d + We_d)$ and Ca_c. The area at and below curves corresponds to dripping regime and the area over curves correspond to jetting regime.

For the continuous phase, the capillary number is mostly chosen to represent the flow maps. For the dispersed phase, choosing either capillary number or Weber number among different chemical systems and different geometry of microchannels, remains as an opened question. Previous study of Utada et al. (2007) in a co-flow microfluidic device, shows that the inertial effects of dispersed phase would dominate the flow regime transition by changing

the flow rates of dispersed phase. However, according to the studies in a flow-focusing microchannel (Zhu et al., 2015; Kovalchuk et al., 2018), they underline that the viscous effects of dispersed phase should be more important for studying flow regime transition. More recently, Kovalchuk et al. (2019) explained that the Reynolds numbers ($Re_d = We_d/Ca_d$) of all the dispersed phases used in their study, are close to 1 for the transition of dripping-to-jetting, so Ca_d rather than We_d should be used.

In our study, Re_d of dibutyl adipate for the transition of dripping-to-jetting is always less than 1 like the cases in the references (Kovalchuk et al., 2018, 2019). Therefore, the critical Ca_d of this dispersed phase for the flow regime transition is comparable to that in the literature. However, for n-butyl acetate, its inertial effects are more important than its viscous effects because the Re_d is much larger than the order of unity, as shown in **Figure 10(a)**. This might indicate that the inertial effects of n-butyl acetate are no more negligible. At least, the inertial effects of the latter dispersed phase should be considered as important as the its viscous effects in this study. If the flow regime transition is influenced by both the inertial and viscous forces of the inner phase, a sum of these forces ($We_d + Ca_d$) should be used to guide the transition (Mak et al., 2017).

Therefore, we plotted the dripping-to-jetting transition as a function of ($Ca_d + We_d$) and Ca_c in **Figure 10(b)**. Despite a shift of the transition lines to larger Ca_c and smaller ($Ca_d + We_d$) after adding 1wt% Tween 80 into the water phase, the transition lines have a good agreement among four systems by using these two parameters. The shift of the transition lines for these systems with Tween 80 is probably due to a decrease of the interfacial tension as Kovalchuk et al. (2019) also observe the same phenomena by adding surfactants. Please note that the noticeable difference of the transition's lines in **Figure 10(b)** for n-butyl acetate comparing to that in **Figure 9**, is owing to the fact that the flow maps represented by Ca_d and Ca_c for n-butyl acetate in **Figure 9** are relatively too sparse. Because of the low viscosity of n-butyl acetate, a little change for Ca_d causes great changes for We_d. Therefore, the transition lines in **Figure 10(b)** for n-butyl acetate are based on its flow maps represented by We_d (**Figure S6**, given in the supplementary material) rather than Ca_d.

5. Conclusions

In this paper, we have presented the study about the influence of wetting properties of different chemical systems, on the establishment of flow regimes within a microchannel. Without adding any surfactant, there is the existence of disordered flow regimes at low flow rates of dispersed and continuous phases, caused by wetting of dispersed phase on the surface of microchannel. Those disordered regimes should be evicted for further encapsulation process.

In the presence of Tween 80, the dynamic interfacial tension within microfluidics depends on the concentration of surfactant in the aqueous phase. The estimated diffusion time of Tween 80 is compared to the droplet formation time at different conditions. A sufficiently large concentration gradient of surfactant micellars, is necessary to reduce the dynamic interfacial tension to its equilibrium value.

Adding surfactant can modify the surface properties (contact angles) of microchannel, however it will also introduce the difficulty of measuring dynamic interfacial tension. Therefore, further investigation about wetting problem by CFD is highly needed, since it becomes easy to decouple the influence of contact angles and interfacial tension. Besides, more dispersed phases with different viscosity should be studied to better understand the relationship between the viscosity of dispersed phases and the flow maps. It would be also useful to discuss choices of the more appropriate dimensionless numbers (Ca_d, We_d or both) to represent flow regimes transition.

Funding

This work was partially funded by the Région Provence-Alpes-Côte d'Azur.

References

Bashir, S., Solvas, X. C. I., Bashir, M., Rees, J. M., and Zimmerman, W. B. J. (2014). Dynamic wetting in microfluidic droplet formation. *Biochip Journal*, 8(2):122–128. doi:10.1007/s13206-014-8207-y.

Chen, P. and Neumann, A. (1998). Derivation of a general kinetic equation for transfer-controlled adsorption at liquid interfaces using statistical rate theory. *Colloids and Surfaces A: Physicochemical and Engineering Aspects*, 143(2):331 – 338. doi:https://doi.org/10.1016/S0927-7757(98)00262-3.

Cho, J.-S., Kwon, A., and Cho, C.-G. (2002). Microencapsulation of octadecane as a phase-change material by interfacial polymerization in an emulsion system. *Colloid and Polymer Science*, 280(3):260–266. doi:10.1007/s00396-001-0603-x.

Diogo, J. C. F., Avelino, H. M. N. T., Caetano, F. J. P., and Fareleira, J. M. N. A. (2014). Density measurements of compressed dipropyl, dibutyl, bis(2-ethylhexyl) adipates from (293 to 373k) at pressures up to about 68mpa. *Fluid Phase Equilibria*, 374:9–19. doi:10.1016/j.fluid.2014.04.018.

Diogo, J. C. F., Avelino, H. M. N. T., Caetano, F. J. P., and Fareleira, J. M. N. A. (2015). Viscosity measurements of compressed liquid dipropyl and dibutyl adipates. *Fluid Phase Equilibria*, 395:26–32. doi:10.1016/j.fluid.2015.03.016.

Donahue, D. J. and Bartell, F. E. (1952). The boundary tension at water-organic liquid interfaces. *The Journal of Physical Chemistry*, 56(4):480–484. doi:10.1021/j150496a016.

Doran, P. M. (2013). *Chapter 10 - Mass Transfer*, pages 379–444. Academic Press, London. doi:https://doi.org/10.1016/B978-0-12-220851-5.00010-1.

Dreyfus, R., Tabeling, P., and Willaime, H. (2003). Ordered and disordered patterns in two-phase flows in microchannels. *Physical Review Letters*, 90(14):144505. doi:https://link.aps.org/doi/10.1103/PhysRevLett.90.144505.

Eastoe, J. and Dalton, J. S. (2000). Dynamic surface tension and adsorption mechanisms of surfactants at the air-water interface. *Adv Colloid Interface Sci*, 85(2-3):103–44. doi: 10.1016/s0001-8686(99)00017-2.

Fu, T., Wu, Y., Ma, Y., and Li, H. Z. (2012). Droplet formation and breakup dynamics in microfluidic flow-focusing devices: From dripping to jetting. *Chemical Engineering Science*, 84(Supplement C):207–217. doi:https://doi.org/10.1016/j.ces.2012.08.039.

Glawdel, T., Elbuken, C., and Ren, C. L. (2012). Droplet formation in microfluidic t-junction generators operating in the transitional regime. i. experimental observations. *Physical Review E*, 85(1):016322. doi:https://link.aps.org/doi/10.1103/PhysRevE.85.016322.

Glawdel, T. and Ren, C. L. (2012). Droplet formation in microfluidic t-junction generators operating in the transitional regime. iii. dynamic surfactant effects. *Physical Review E*, 86(2):026308. doi:https://doi.org/10.1103/PhysRevE.86.026308.

Glenn, K. M., Moroze, S., Bhattacharya, S. C., and Palepu, R. M. (2005). Effect of ethylene glycol on the thermodynamic and micellar properties of tween 40, 60, and 80. *Journal of Dispersion Science and Technology*, 26(1):79–86. doi:10.1081/DIS-200040137.

Jacquemond, M., Jeckelmann, N., Ouali, L., and Haefliger, O. (2009). Perfume-containing polyurea microcapsules with undetectable levels of free isocyanates. *Journal of Applied Polymer Science*, 114:3074 – 3080. doi:10.1002/app.30857.

Ji, H., Long, Q., He, Y., and Yao, X. (2010). Palladium nanoclusters entrapped in polyurea: A recyclable and efficient catalyst for reduction of nitro-benzenes and hydrodechlorination of halogeno-benzenes. *Science China Chemistry*, 53(7):1520–1524. doi:10.1007/s11426-010-4027-7.

Joos, P. and Uffelen, M. (1995). Theory on the growing drop technique for measuring dynamic interfacial tension. *Journal of Colloid and Interface Science - J COLLOID INTERFACE SCI*, 171:297–305. doi:10.1006/jcis.1995.1184.

Jose, B. M. and Cubaud, T. (2014). Formation and dynamics of partially wetting droplets in square microchannels. *RSC Advances*, 4(29):14962–14970. doi:10.1039/C4RA00654B.

Kovalchuk, N. M., Roumpea, E., Nowak, E., Chinaud, M., Angeli, P., and Simmons, M. J. H. (2018). Effect of surfactant on emulsification in microchannels. *Chemical Engineering Science*, 176:139–152. doi:https://doi.org/10.1016/j.ces.2017.10.026.

Kovalchuk, N. M., Sagisaka, M., Steponavicius, K., Vigolo, D., and Simmons, M. J. H. (2019). Drop

formation in microfluidic cross-junction: jetting to dripping to jetting transition. *Microfluidics and Nanofluidics*, 23(8):103. doi:10.1007/s10404-019-2269-z.

Li, D., Li, X., Chen, C., Zheng, Z., and Chang, H. (2018). Monodisperse water-in-oil-in-water emulsions generation for synthesising alginate hydrogel microspheres via locally hydrophobic modification to pmma microchannels. *Sensors and Actuators B: Chemical*, 255:1048–1056. doi:https://doi.org/10.1016/j.snb.2017.08.152.

Li, W., Nie, Z. H., Zhang, H., Paquet, C., Seo, M., Garstecki, P., and Kumacheva, E. (2007). Screening of the effect of surface energy of microchannels on microfluidic emulsification. *Langmuir*, 23(15):8010–8014. doi:10.1021/la7005875.

Liang, C., Lingling, X., Hongbo, S., and Zhibin, Z. (2009). Microencapsulation of butyl stearate as a phase change material by interfacial polycondensation in a polyurea system. *Energy Conversion and Management*, 50(3):723 – 729. doi:https://doi.org/10.1016/j.enconman.2008.09.044.

Lone, S., Lee, H. M., Kim, G. M., Koh, W.-G., and Cheong, I. W. (2013). Facile and highly efficient microencapsulation of a phase change material using tubular microfluidics. *Colloids and Surfaces A: Physicochemical and Engineering Aspects*, 422(Supplement C):61–67. doi:https://doi.org/10.1016/j.colsurfa.2013.01.035.

Léonard-Akkari, L., Guégan, S., Courand, F., Couvert, O., Lepage, J.-F., Rondeau-Mouro, C., Desriac, N., Mathot, A.-G., Leguérinel, I., Coroller, L., and Decourcelle, N. (2018). Dispersed phase volume fraction, weak acids and tween 80 in a model emulsion: Effect on the germination and growth of bacillus weihenstephanensis kbab4 spores. *Food Research International*, 109:288 – 297. doi:https://doi.org/10.1016/j.foodres.2018.04.016.

Mak, S. Y., Chao, Y., and Shum, H. C. (2017). The dripping-to-jetting transition in a co-axial flow of aqueous two-phase systems with low interfacial tension. *RSC Advances*, 7(6):3287–3292. doi:10.1039/C6RA26556A.

Paria, S. and Khilar, K. C. (2004). A review on experimental studies of surfactant adsorption at the hydrophilic solid–water interface. *Advances in Colloid and Interface Science*, 110(3):75–95. doi:https://doi.org/10.1016/j.cis.2004.03.001.

Polenz, I., Datta, S. S., and Weitz, D. A. (2014). Controlling the morphology of polyurea microcapsules using microfluidics. *Langmuir*, 30(44):13405–10. doi:10.1021/la503234z.

Polenz, I., Weitz, D. A., and Baret, J. C. (2015). Polyurea microcapsules in microfluidics: surfactant control of soft membranes. *Langmuir*, 31(3):1127–34. doi:10.1021/la5040189.

Ranz, W. E. and Marshall, W. R. (1952). Evaporation from drops. *Chemical Engineering Progress*, 48(3):141–146.

R.LIDE, D. (2009). Crc handbook of chemistry and physics, 2009-2010, 90th edition. *Journal of the American Chemical Society*, 131(35):12862–12862. doi:10.1021/ja906434c.

Roberts, C. C., Rao, R. R., Loewenberg, M., Brooks, C. F., Galambos, P., Grillet, A. M., and Nemer, M. B. (2012). Comparison of monodisperse droplet generation in flow-focusing devices with hydrophilic and hydrophobic surfaces. *Lab on a Chip*, 12(8):1540–1547. doi:10.1039/C2LC21197A.

Romero, P. A. and Abate, A. R. (2012). Flow focusing geometry generates droplets through a plug and squeeze mechanism. *Lab on a Chip*, 12(24):5130–5132. doi:10.1039/C2LC40938K.

Rotem, A., Abate, A. R., Utada, A. S., Van Steijn, V., and Weitz, D. A. (2012). Drop formation in non-planar microfluidic devices. *Lab Chip*, 12(21):4263–8. doi:10.1039/c2lc40546f.

Scarfato, P., Avallone, E., Iannelli, P., De Feo, V., and Acierno, D. (2007). Synthesis and characterization of polyurea microcapsules containing essential oils with antigerminative activity. *Journal of Applied Polymer Science*, 105(6):3568–3577. doi:10.1002/app.26420.

Sumner, A. L., Menke, E. J., Dubowski, Y., Newberg, J. T., Penner, R. M., Hemminger, J. C., Wingen, L. M., Brauers, T., and Finlayson-Pitts, B. J. (2004). The nature of water on surfaces of laboratory systems and implications for heterogeneous chemistry in the troposphere. *Physical Chemistry Chemical Physics*, 6(3):604–613. doi:10.1039/B308125G.

Szymczyk, K. and Taraba, A. (2016). Aggregation behavior of triton x-114 and tween 80 at various temperatures and concentrations studied by density and viscosity measurements. *Journal of Thermal Analysis*

and Calorimetry, 126(1):315–326. doi:10.1007/s10973-016-5631-3.

Tostado, C. P., Xu, J. H., and Luo, G. S. (2011). The effects of hydrophilic surfactant concentration and flow ratio on dynamic wetting in a t-junction microfluidic device. *Chemical Engineering Journal*, 171(3):1340–1347. doi:10.1016/j.cej.2011.05.043.

Utada, A. S., Fernandez-Nieves, A., Gordillo, J. M., and Weitz, D. A. (2008). Absolute instability of a liquid jet in a coflowing stream. *Phys Rev Lett*, 100(1):014502. doi:10.1103/PhysRevLett.100.014502.

Utada, A. S., Fernandez-Nieves, A., Stone, H. A., and Weitz, D. A. (2007). Dripping to jetting transitions in coflowing liquid streams. *Phys Rev Lett*, 99(9):094502. doi:10.1103/PhysRevLett.99.094502.

Wang, K., Lu, Y. C., Xu, J. H., and Luo, G. S. (2009). Determination of dynamic interfacial tension and its effect on droplet formation in the t-shaped microdispersion process. *Langmuir*, 25(4):2153–2158. doi:10.1021/la803049s.

Welty, J. R., Wicks, C. E., and Wilson, R. E. (1969). *Chapter 30 - Convective Mass Transfer Correlations*, pages 617–654. Wiley.

Wu, N., Zhu, Y., Leech, P. W., Sexton, B. A., Brown, S., and Easton, C. (2007). Effects of surfactants on the formation of microdroplets in the flow focusing microfluidic device. In *BioMEMS and Nanotechnology III*, volume 6799, pages 98 – 105. International Society for Optics and Photonics, SPIE. doi:10.1117/12.769326.

Xu, J. H., Dong, P. F., Zhao, H., Tostado, C. P., and Luo, G. S. (2012). The dynamic effects of surfactants on droplet formation in coaxial microfluidic devices. *Langmuir*, 28(25):9250–9258. doi:10.1021/la301363d.

Xu, J. H., Luo, G. S., Li, S. W., and Chen, G. G. (2006). Shear force induced monodisperse droplet formation in a microfluidic device by controlling wetting properties. *Lab Chip*, 6:131–136. doi:10.1039/B509939K.

Yao, C. Q., Liu, Y. Y., Xu, C., Zhao, S. N., and Chen, G. W. (2018). Formation of liquid-liquid slug flow in a microfluidic t-junction: Effects of fluid properties and leakage flow. *Aiche Journal*, 64(1):346–357. doi:10.1002/aic.15890.

Yoon, D. H., Tanaka, D., Sekiguchi, T., and Shoji, S. (2018). Structural formation of oil-in-water (o/w) and water-in-oil-in-water (w/o/w) droplets in pdms device using protrusion channel without hydrophilic surface treatment. *Micromachines*, 9(9). doi:10.3390/mi9090468.

Yu, J.-Q., Wu, H.-C., Ramarao, C., Spencer, J. B., and Ley, S. V. (2003). Transfer hydrogenation using recyclable polyurea-encapsulated palladium: efficient and chemoselective reduction of aryl ketones. *Chem. Commun.*, pages 678–679. doi:10.1039/B300074P.

Zhan, S., Chen, S., Chen, L., and Hou, W. (2016). Preparation and characterization of polyurea microencapsulated phase change material by interfacial polycondensation method. *Powder Technology*, 292:217 – 222. doi:https://doi.org/10.1016/j.powtec.2016.02.007.

Zhu, P., Kong, T., Kang, Z., Tian, X., and Wang, L. (2015). Tip-multi-breaking in capillary microfluidic devices. *Sci Rep*, 5:11102. doi:10.1038/srep11102.

Zhu, P. and Wang, L. (2017). Passive and active droplet generation with microfluidics: a review. *Lab on a Chip*, 17(1):34–75. doi:10.1039/C6LC01018K.